JPE 16-2-33

http://dx.doi.org/10.6113/JPE.2016.16.2.748
ISSN(Print): 1598-2092 / ISSN(Online): 2093-4718

A Control and Protection Model for the Distributed Generation and Energy Storage Systems in Microgrids

Makarand Sudhakar Ballal[†], Kishor V. Bhadane[*], Ravindra M. Moharil[*], and Hiralal M. Suryawanshi[**]

[†,**]Department of Electrical Engineering, Visvesvaraya National Institute of Technology, Nagpur, India
[*]Department of Electrical Engineering, Yeshwantrao Chavan Collage of Engineering, Nagpur, India

Abstract

The microgrid concept is a promising approach for injecting clean, renewable, and reliable electricity into power systems. It can operate in both the grid-connected and the islanding mode. This paper addresses the two main challenges associated with the operation of a microgrid i.e. control and protection. A control strategy for inverter based distributed generation (DG) and an energy storage system (ESS) are proposed to control both the voltage and frequency during islanding operation. The protection scheme is proposed to protect the lines, DG and ESS. Further, the control scheme and the protection scheme are coordinated to avoid nuisance tripping of the DG, ESS and loads. The feasibility of the proposed method is verified by simulation and experimental results.

Key words: Distributed Generation (DG), Energy Storage System (ESS), Microgrid, Islanding

I. INTRODUCTION

To meet the challenges of integrating various distributed generations (DGs) and energy storage systems (ESSs) into power systems, the microgrid concept is a promising approach [1]-[2]. Both grid-connected and islanded operations of a microgrid are possible [3]. A microgrid can either inject power into, or absorb power from, the main grid, when it performs grid-connected operations. The main grid maintains the supply–demand balance most of the time [4]. In the islanded mode, highly intermittent renewable generators (RG) and various load demands pose new challenges to the optimal resource management of a microgrid [5]. Distributed generation encompasses a wide range of prime mover technologies, such as internal combustion (IC) engines, gas turbines, micro-turbines, photovoltaics, fuel cells and wind power. A microgrid involves a low voltage electrical grid, loads, storage devices and a hierarchical management and control scheme supported by a communication system.

Manuscript received Jul. 13, 2015; accepted Oct. 23, 2015
Recommended for publication by Associate Editor Il-Yop Chung.
[†]Corresponding Author: msb_ngp@rediffmail.com
Tel: +91-712-2801147, Fax: +91-712-2223230, Visvesvaraya National Institute of Technology
[*]Dept. of Electrical Eng., Yeshwantrao Chavan Collage of Eng., India
[**]Dept. of Electrical Eng., Visvesvaraya Nat'l Inst. of Tech., India

Microgrid has good environmental and economic benefits and they have attracted the attentions of more and more power researchers [6]–[8]. The microgrid advantages are as follows: (i) They provide a good solution for supplying power in case of an emergency and power shortage during power interruptions in the main grid. (ii) Plug and play functionality is featured for switching to a suitable mode of operation. This is true for both grid connected or islanded operation. This functionality also provides voltage and frequency protection during islanded operation and capability to resynchronize safely while connecting the microgrid to the grid. (iii) Microgrids can independently operate without connecting to the main grid during the islanding mode. All of the loads have to be supplied and shared by DGs. In addition, microgrids also allow for the integration of renewable energy sources such as photovoltaic, wind and fuel cell generations [9]-[11].

An adaptive critic-based control structure for the power control of grid connected microgrids is presented in [12]. The control system consists of a neuro-fuzzy controller and it modifies its behavior so that the critic's satisfaction is insured. However, islanded mode control is not considered in it. An enhanced power sharing scheme for islanding microgrids is described in [13]. A method that utilizes the frequency droop as a link to compensate reactive, imbalance, and harmonic power sharing errors are discussed in [14]. To realize better

TABLE I
COMPARISON BETWEEN EXISTING AND PROPOSED METHOD

SN	Criterion	Existing method	Proposed method
1	Integrated Controls	No	Yes
2	Fault tolerant controls for safety redundancy	No	Yes
3	DC coupled system	No	Yes
4	Stability performance	No	Yes
5	Perturbation to the disturbance	Yes	Improved
6	Islanding detection	Yes	Improved
7	Experimentation Validation	Possible	Improved

compensation performance, independent harmonic power-sharing error compensation at each harmonic order and sequence can be developed. The islanding search sequence techniques were implemented to control active–reactive power control, maximum power point tracking (MPPT) algorithm, and phase-locked loop routine as described in [15]. However, the suggested optimized detection time is about 250 ms, and the voltage collapse below is 30 V.

The frequency of a microgrid may change rapidly and frequently due to the unexpected supply–demand imbalance and small inertia present in microgrids. There is an increasing need to develop fast, flexible, reliable, and cost-effective distributed solutions to meet the requirements of the real-time applications in microgrids, particularly under the high penetration level of RG [16]-[17]. In [18] islanding operation, unbalanced reactive power versus negative-sequence conductance and the droop between the harmonic power versus the harmonic conductance have been described. The cooperative control for the power quality enhancement in microgrids can be implemented.

The role of self-organizing dynamic agent network equipped with a decentralized consensus protocols in smart microgrid synchronization, estimation, monitoring, and control is discussed in [19]. However, it is possible that the dynamic agents can effectively solve these problems in the presence of highly variable load and generation conditions. A methodology to characterize the interactions between a distribution network operator and clusters of microgrids is described in [20]. A bi-level stochastic formulation is developed to model the problem of taking into account the strategic behaviors of all entities and intermittent outputs of DGs. The multi-agent application of substation protection coordination with DGs is discussed in [21].

This paper targets small-scale self-contained medium voltage microgrid systems, which are composed of DG, ESS, utility supply and loads.

A fully distributed algorithm based on a multi agent system (MAS) framework is proposed to maximize the overall welfare of all the participants. In this paper, a control and protection scheme is proposed for inverter based DG and ESS microgrid operations. Three issues are addressed in this work:

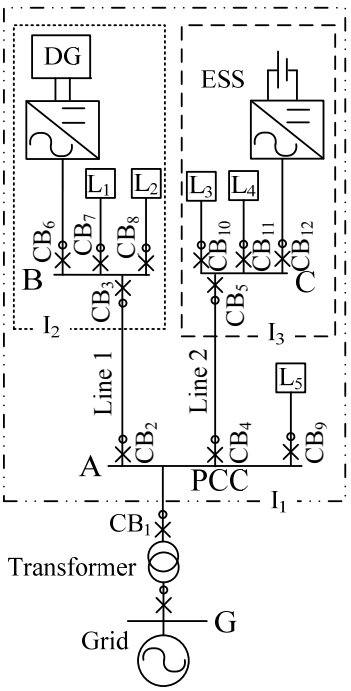

Fig. 1. System under study.

1. Designing a DG and ESS interface control strategy for both grid-connected and islanded operation.
2. Line, DG and ESS protection during grid connected and islanded operation.
3. Coordination between the control scheme and the protection scheme to avoid nuisance tripping of the DG, ESS and non-critical loads while maintaining safe operation.

A comparison between the existing and proposed methods is given in Table I. The rest of this paper is organized as follows: Section II presents the system under study and the different scenarios studied. Section III presents the proposed control and protection scheme for the inverter based DG and ESS for grid connected microgrid operation. Section IV provides simulation and experimental results. The last section draws some conclusions.

II. SYSTEM UNDER STUDY

The system under study is of 20 kVA, three-phase, 400 volt, 50 Hz system consisting of an inverter based DG and ESS (battery) as shown in Fig. 1. The system features are given in Table II. The local utility grid is connected and the loads on the system are divided into critical and non critical loads. The loss of electric power means an interruption of some applications such as vital digital communications networks, advanced medical therapies, financial transactions such as credit cards and bank operations, vital transportation such as elevator service, refrigeration of sensitive biological experiments and other essential services. The vital aspect of such functionality creates a demand for non-stop electric power. The phrase “non-stop” in this discussion is meant to describe loads that

cannot endure even a brief loss of power. These kinds of loads are termed as "critical loads." The critical loads have also given priority. In this study L_1 and L_4 are critical loads having top priority. Whereas, the remaining loads are all non-critical loads.

The active power rating of the critical loads are chosen so that the ESS is capable of supplying power without exceeding its capacity for a predefined time interval during islanding operation. Each line is equipped with an over current relay to protect the lines from line faults. In addition, the DG and ESS are equipped with their respective islanding detection schemes. In order to assure safe and efficient operation of the designed control and protection scheme during normal and islanding operation, several conditions were studied. These configurations are as follows.

(i) Normal operation, i.e. the DG and ESS are working in parallel with the utility. The ESS is operating under the floating mode. Part of the active and the entire reactive power management is made by the utility.

(ii) Microgrid islanding (I_1), i.e. the DG and ESS are working in parallel. Utility is disconnected and the DG supplies reactive power.

(iii) DG islanding (I_2), i.e. the DG is working separately from combination of the utility and the ESS.

(iv) ESS islanding (I_3), i.e. the ESS is operating individuallyapart from a combination of the utility and the DG.

(v) Two separate islanding (I_2 and I_3), i.e. the DG and ESS are operating separately without connected to the utility.

III. Proposed Control and Protection Scheme

The microgrid considered in this paper consists of a multi agent system for making several autonomous decisions. Each agent represents a major autonomous component of the microgrid. The agents can monitor and control the corresponding components. They can also communicate with other agents. Each source or load makes decisions locally. This can potentially create a distributed, scalable and robust control for the microgrid. To implement a multi-agent system control framework, it is necessary to define the functions of each agent according to their characteristics and goals. The objectives and responsibilities of each agent in the multi-agent system are discussed below [23].

1. Power Production Agent: It is responsible for monitoring, controlling and negotiating the power produced by the corresponding micro-source and its ON/OFF status.

2. Load or Consumption Agent: It is capable of monitoring, controlling and negotiating the power level of a controllable load and its connection status. It is also capable of shuttng off based on the amount of available power, especially when the microgrid is in the islanded mode. The multi-agent system has separate load agents for critical and non-critical loads.

3. ESS Agent: It monitors its charging level and requests power from the micro-source agent and the power grid agent when this level is low based on the locally measured information. The local control of the ESS determines how much energy needs to be stored or supplied at every instant.

4. PCC Agent: It monitors the grid voltage, phase-angle and frequency. It is also responsible for informing the other agents of changes in the microgrid status.

5. Grid Agent: It is responsible for monitoring and negotiating power from the micro-sources and exporting power when the microgrid is in the grid-connected mode. The power export from the main grid is according to the market operation.

6. CB Agent: It interacts with the corresponding circuit breaker of the microgrid, and is capable of working as a switch. The circuit breaker agent can lead to the connection or disconnection of a DG and/or an ESS or a load based on the control commands.

7. Bus Agent: It monitors the voltage magnitude and phase angle, and maintains voltage that does not exceed its limits. The proposed architecture has AC bus agents.

8. Microgrid Central Controller Agent: It represents the microgrid model in a multi-agent system. In addition, the multi-agent system has a distributed database. It is required to keep the messages and data shared between the agents, and to keep track of each agent. It may also serve as a data access point for the agents.

Therefore, the multi-agent system provides a flexible protection alternative. It also sheds non-critical loads according to a pre-defined prioritized list while stabilizing a microgrid after its isolation from the main grid. The protection and control scheme should be coordinated to minimize nuisance tripping of the DG, ESS and loads while keeping both the voltage and the frequency within standard levels. This section presents the proposed control and protection scheme adopted for both the grid connected and islanded operation of a

TABLE II
System Features

DG Inverter 1 rated power	5 kVA
ESS Inverter 2 rated power	3 kVA
ESS Battery rated capacity	48 kWh
Battery inverter output inductance L1	3 mH
ESS Battery rated voltage	240 volts
RMS value of the inverter output voltage E	230 volts
Droop coefficient M_P	0.3 Hz.
Minimum frequency deviation Δf_{min}	0.5 Hz
Maximum frequency deviation Δf_{max}	2.0 Hz
Impedance of Line 1 in Ohms	(1/25+j 1/40)
Impedance of Line 2 in Ohms	(1/60+j 1/80)
Load L_1 in kVA	2+j0
Load L_2 in kVA	2+j1
Load L_3 in kVA	5+j2
Load L_4 in kVA	2+j0
Load L_5 in kVA	8+j4

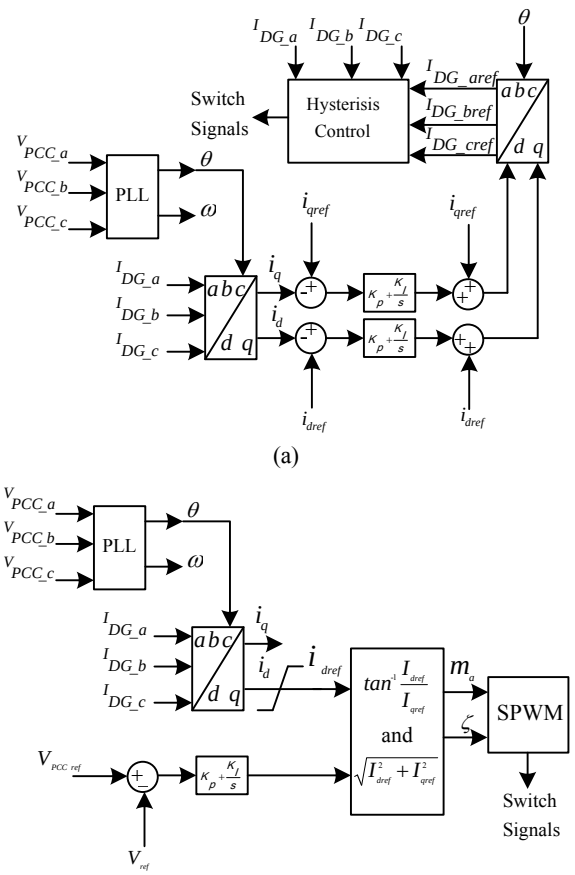

Fig. 2. Block diagram of (a) Current controlled inverter with Hysteresis PWM and (b) P-V controlled inverter with sinusoidal PWM.

microgrid and the different islanded operations produced under fault conditions.

A. Proposed Control Scheme

The interface control is responsible for controlling the DG active and reactive power output. It is most commonly designed to operate at a unity power factor to avoid interference with the voltage regulation devices connected on the utility side. To achieve this, the DG interface control implemented during grid-connected operation is designed to supply active power only. The load's reactive power requirement is supplied by the utility. Fig. 2(a) presents a block diagram of the interface control during grid-connected operation. The *a-b-c* current components are transformed using Park's Transformation to their direct axis (I_d) and quadrature axis (I_q) components. For unity power factor operation, I_{qref} is set to zero.

Unfortunately, this interface control is not capable of maintaining the voltage and frequency within permissible levels, especially for critical loads with reactive power requirements, during micro-grid operation. Since the DG and ESS is no longer connected to the utility during islanded operation, operating the DG to supply reactive power will have

TABLE III
CONTROL STRATEGY

System Status	Circuit Breaker OFF	Control Action
Normal operation	Nil	DG : PQ Control ESS : PQ Control
Microgrid islanded operation	CB_1 CB_9 CB_{10}	DG : PV Control ESS : PQ Control
Islanded operation of DG	CB_2 CB_3 CB_8	DG : PV Control ESS : PQ Control
Islanded operation of ESS	CB_4 CB_5 CB_{10}	DG : PQ Control ESS : PV Control
Islanded operation of DG and ESS	CB_2 CB_3 CB_4 CB_5 CB_8 CB_9 CB_{10}	DG : PV Control ESS : PV Control

no impact on the utility voltage regulation devices. Thus, the interface control is designed to maintain the voltage by supplying reactive power during islanded operation. Each interface control is equipped with a second control strategy as shown in Fig. 2(b). The DG is designed to supply active power and to maintain the voltage at the DG bus at 1 p.u. The algorithm is depicted in Fig. 3.

In order to manage and control the DG and ESS under different possible scenarios, a Central Processing Unit (CPU) is implemented. Table III presents the control strategy used for operating the DG and ESS under different system configurations. The CPU receives signals from the islanding algorithm incorporated with the DG and ESS. Based on the received signal, the CPU sends out signals to the DG and ESS to specify the mode of operation and to the circuit breakers to specify their status. In this paper, a simple passive islanding scheme has been implemented which relies on voltage [22].

This control and protection algorithm has two objectives. The first objective is to provide effective control so that the operation maximizes the utilization of each component in the system. The second objective is to provide protection under abnormal situations. In order to maximize the utilization of each component in the microgrid, it is necessary to identify the states of the system. The five states in this system are 1) the normal condition, 2) microgrid islanding, 3) DG islanding, 4) ESS islanding and 5) DG/ESS islanding. The stability of the system is a critical concern and a priority. Since the frequency takes time to stabilize, a delay of 300 m sec is incorporated by the algorithm. The algorithm initially reads the status of the circuit breakers (CB), the voltages at all of the buses, and the flow of currents from the utility, the DG and the ESS. Thereby, it is possible to identify the state of the system.

It can be seen that the control action is based only on rate of change of the voltage deviation of the DG and the ESS. During normal operation, the voltage measured at buses B and C remain within their permissible levels, and the output of the islanding detection for the DG and ESS will not come into existence. If the utility is disconnected, a voltage and frequency

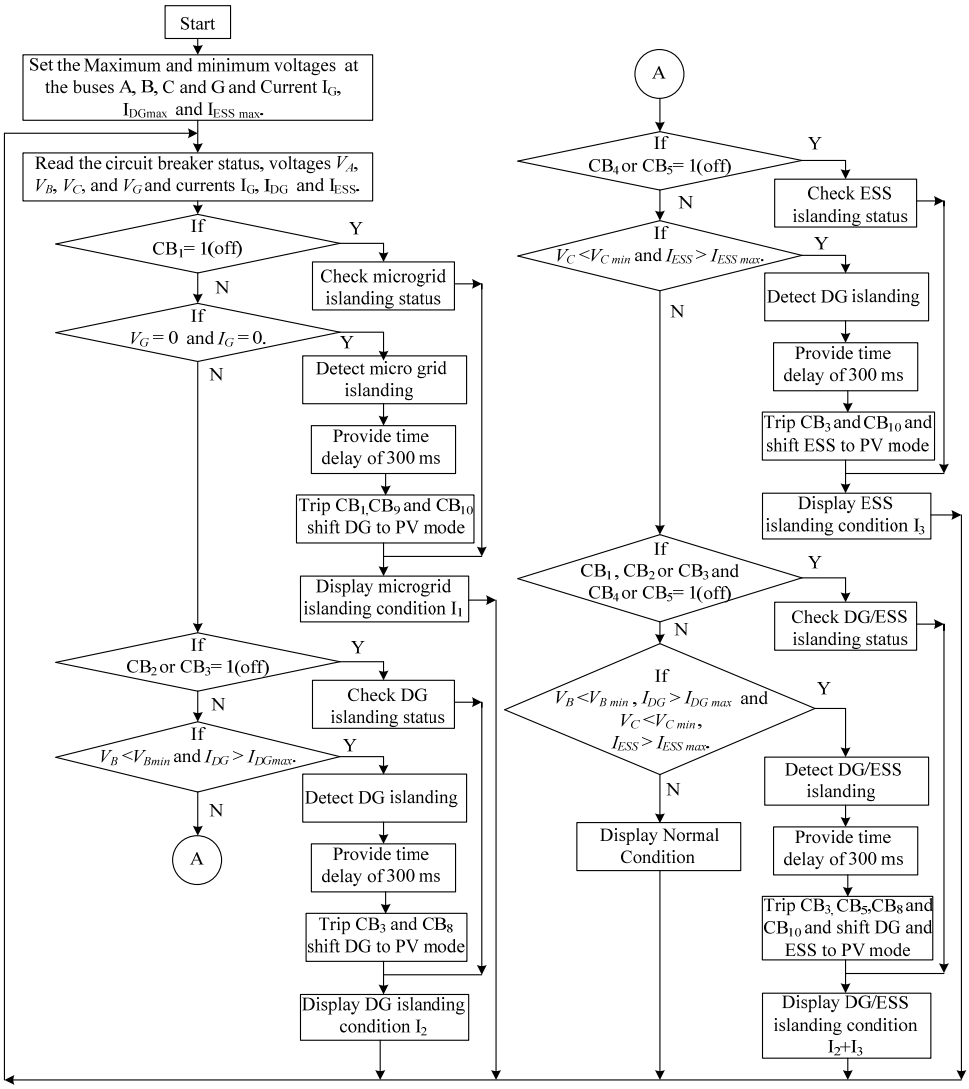

Fig. 3. Control and protection algorithm.

deviation will occur at these buses.

In this case, since some of the loads require reactive power, the DG and the ESS cannot operate at a unity power factor. If CB_1 is off, the microgrid islanding status is directly confirmed; otherwise if the voltage at bus G, i.e. V_G, becomes zero and the current I_G is also zero, and if they remain zero after a time delay of 300 ms, microgrid islanding is detected. Immediately after this time delay, the non-critical loads L_3 and L_5 are curtailed by opening CB_9 and CB_{10}. This is the microgrid islanding condition situation (I_1). The DG control is now shift over to the PV mode and supplies to remaining connected loads with the ESS.

If CB_2 or CB_3 is off due to a fault on line 1, this is a DG islanding status. This status also gets detected, if $V_B < V_{B\ min}$ and $I_{DG} > I_{DG\ max}$. If theses parameters remain under these constraints after a time delay of 300 ms, the DG starts to operate in the PV mode and only supplies to the critical load L_1, whereas the load L_2 is shaded by opening CB_8. This is DG islanding (I_2) and it works independently from the remaining power system. Similarly, if CB_4 or CB_5 is off due to a fault on line 2, this is an ESS islanding status. This status also gets confirmed, if $V_C < V_{C\ min}$ and $I_{ESS} > I_{ESS\ max}$.

If theses parameters remain under these constraints after a time delay of 300 ms, the ESS starts to operate in the PV mode and only supplies to the critical load L_4. This is ESS islanding (I_3) and it also works independently from the remaining power system. The algorithm, continuously reads the circuit breakers status, the voltages of all the buses and the flow of the currents. If CB_1, CB_2 or CB_3, CB_4 or CB_5 are off, this indicates two different islanding modes i.e. the DG islanding (I_2) and the ESS islanding (I_3) conditions. These islanding status also get detected when a fault occurs on any of the lines during microgrid operation, if $V_B < V_{Bmin}$ and $I_{DG} > I_{DGmax}$ for the DG islanding condition and $V_C < V_{C\ min}$ and $I_{ESS} > I_{ESS\ max}$ for the ESS islanding condition.

If all theses voltage and current parameters remain under these constraints after a time delay of 300 ms, the DG and the

TABLE IV
OVER CURRENT RELAY SETTINGS

Relay connected at CB location	Current setting p.u.	Time setting
CB_1, CB_6 and CB_{12}	1.1	120 m sec
CB_7 and CB_{11}	1.08	110 m sec
CB_2,CB_3,CB_4 and CB_5	1.05	150 m sec
CB_8,CB_9,and CB_{10}	1.03	100 m sec

TABLE V
VOLTAGE RELAY SETTINGS

Protection function	Voltage p.u. setting	Time setting
Over voltage (V >>)	1.2	100 m sec
Over voltage (V >)	1.08	1 min
Under voltage (V <)	0.8	3 sec

ESS start to operate separately in the PV mode and only supply to critical load L_1 and L_4, respectively. Load L_2 is shaded by the opening CB_8. This generates the conditions for two independent islanding modes, i.e. DG islanding (I_2) and ESS islanding (I_3).

The proposed control strategy is coordinated with a protection scheme to avoid nuisance tripping of the DG, ESS and non-critical loads. In addition, the frequency or voltage exceeds the thresholds for a predefined time, the DG should be disconnected. This will be explained in detail in the next subsection.

B. Proposed Protection Scheme

The second major challenge addressed in this article is microgrid protection. The protection scheme must protect the lines, DG and ESS during the grid connected and islanding operations of the DG and/or the ESS. Over current relay protection is employed and their current and time settings for the relevant load, line and source are depicted in Table IV.

The recommended protection settings provided for the protection unit at the point of common coupling (PCC) i.e. bus A and the generating units are presented in Table V. Once the difference exceeds certain threshold value, both of the breakers on the line are tripped. In addition, each DG is equipped with over/under voltage and frequency protection. The islanding detection algorithm has two main tasks.

1. Identify the type of islanding condition (microgrid, DG or ESS) and send a signal to the CPU to take proper action.

2. Disconnect the DG and/or the ESS if the voltage is not within permissible limits for a predefined time.

For the protection scheme to operate properly, the line and DG/ESS islanding protection must be coordinated. For a fault on one of the lines, the sequence events should be as follows.

1. The over current relays should operate to disconnect the faulted line.

2. After a predefined time delay, chosen to assure that the system has reached a steady state operating point, the CPU sends signals specifying the status of each circuit breaker and the DG/ESS interface control to be used.

3. If after an additional time delay, the islanding detection algorithm still senses an abnormal operating condition, the DG is disconnected and the critical load L_4 is supplied by the ESS. The lines over current relays were designed to operate in 100 - 150 m sec, and a coordination time interval of 150 m sec was used so that the islanding detection algorithm does not operate before the line protection. Thus, the minimum allowable time before the islanding detection algorithm can send a signal to the CPU is 250 m sec.

In addition, a delay in the islanding detection operation was deliberately introduced to accurately determine the configuration of the system. Lastly, if the frequency or voltage of any DG or ESS is not within its permissible level for more than 500 m sec, the DG is disconnected and the critical load is supplied by the ESS.

IV. SIMULATION AND EXPERIMENTAL RESULTS

In this section, the effectiveness of the proposed controller is evaluated. The system given in Fig. 1 and the algorithm shown in Fig. 3 were implemented and simulated in the commercially available software MATLAB. Experimentation is also carried out in the laboratory. It is presented and compared with the simulation cases.

A. Simulation Results

In order to analyze the performance of the proposed control and protection schemes, the different scenarios presented in section II are simulated.

1) Normal Operation: In this scenario, both the DG and the ESS are operated in parallel with the utility. Fig. 4, Fig. 5 and Fig. 6 illustrate the simulation results. It can be seen that the DG supplies approximately 5 kW and zero reactive power. This is because the DG is designed to operate at a unity power factor during normal operation. The ESS is operating under the floating condition. It is neither supplying power nor drawing power. This indicates that the battery of the ESS is completely charged.

The utility fulfills the needs of the remaining active and the entire reactive load. The frequency at bus B and bus C is approximately 50 Hz and the voltage is approximately 1 p.u. All of the circuit breakers are in the closed position and no trip signal is sent to any of the circuit breakers for opening. This is illustrated in Fig. 6.

2) Microgrid Operation: In order to simulate microgrid operation, circuit breaker CB_1 was opened at t = 3.5 seconds. The DG was operating under unity power factor and the ESS was operating under the floating condition prior to the disconnection of the utility power supply.

The obtained simulation results are shown in Fig. 7, Fig. 8 and Fig. 9 for the microgrid condition. As soon as the utility supply is disconnected, both the voltage and frequency deviate

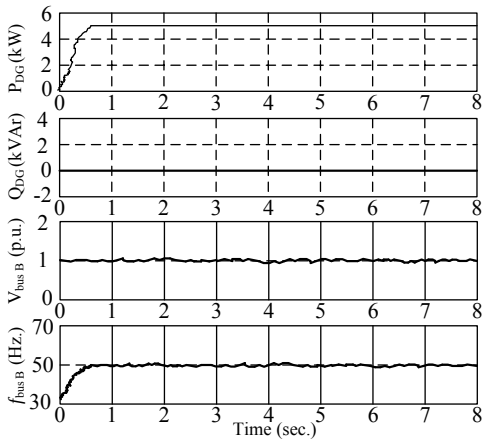

Fig. 4. Results of DG under normal condition for active power, reactive power, voltage and frequency at bus B.

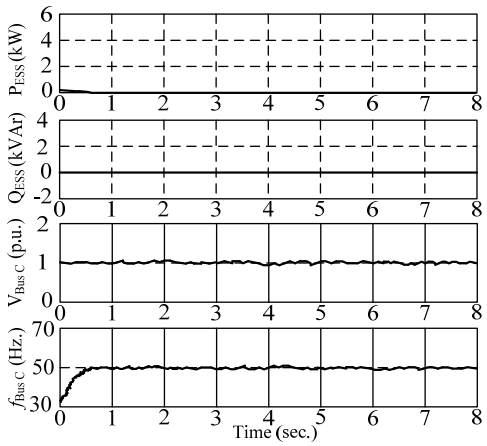

Fig. 5. Results of ESS under normal condition for active power, reactive power, voltage and frequency at bus C.

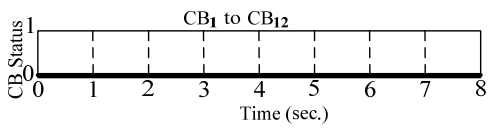

Fig. 6. Status of circuit breakers under normal condition.

due to the excess loading on the DG and ESS. Once the DG and ESS get separated from the utility power supply the first islanding condition (I_1) is experienced by both of them. At this instant, t = 3.5 seconds, the voltage and frequency deviate at bus B and bus C. It can be seen that both the DG and the ESS under the islanding condition experience a frequency and voltage deviation. After 300 m sec, since the frequency at both buses (bus B and bus C) still exceeds the threshold value, the CPU sends a signal to the DG to operate in the P-V controlled mode, while control strategy of the ESS remains unchanged. A 300 m sec time delay was chosen to provide sufficient time for the frequency and voltage to stabilize. In addition, signals are sent to disconnect the non-critical loads (L_3 and L_5) of this islanded region. The decision to perform a change in the control strategy and to disconnect the non-critical loads is taken after 300 m sec. It can be seen that the DG takes approximately

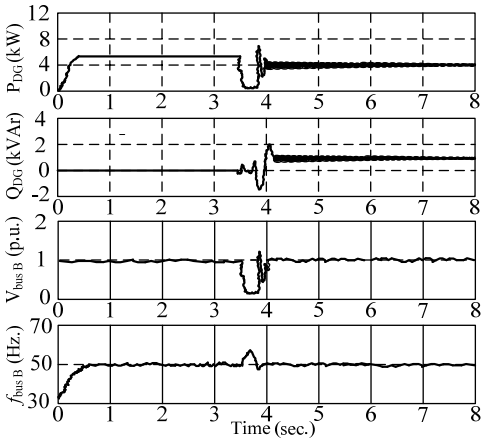

Fig. 7. Results of DG under microgrid condition for active power, reactive power, voltage and frequency at bus B.

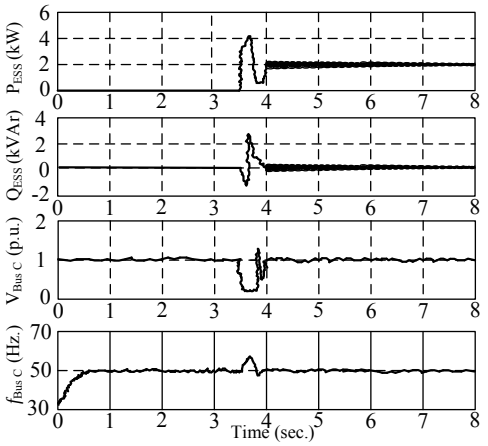

Fig. 8. Results of ESS under normal condition for active power, reactive power, voltage and frequency at bus C.

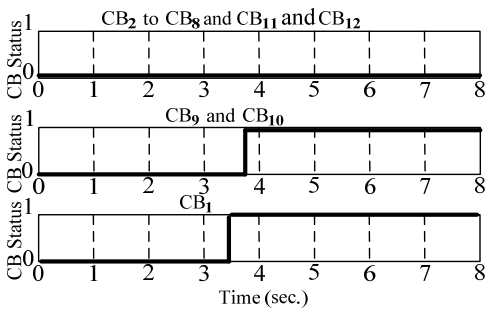

Fig. 9. Status of circuit breakers under microgrid scenario.

an additional 250 m sec and the ESS takes approximately an additional 200 m sec to reach stable operation. The DG is supplying 4 kW and the ESS is supplying 2 kW, the total amount of active power required by the microgrid critical loads.

Since the control of the ESS, is unchanged, the reactive power supplied by it is zero. The stable operation of the microgrid is attributed to the capability of the DG to supply reactive power. By operating the DG as P-V controlled, the critical load reactive power requirements can be satisfied. As shown in Fig. 7, the DG is supplying approximately 1 kVAR,

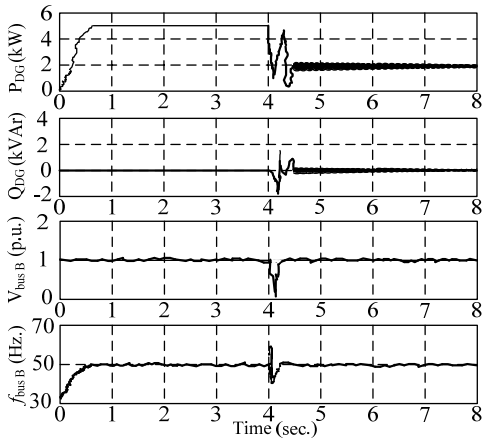

Fig. 10. Results of DG under normal condition when fault occurs at line 1for active power, reactive power, voltage and frequency at bus B.

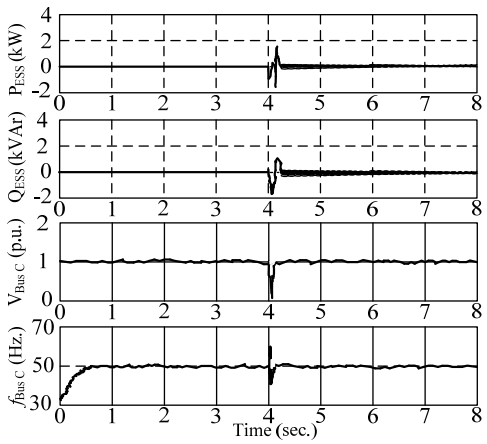

Fig. 11. Results of ESS under normal condition when fault occurs at line 1for active power, reactive power, voltage and frequency at bus C.

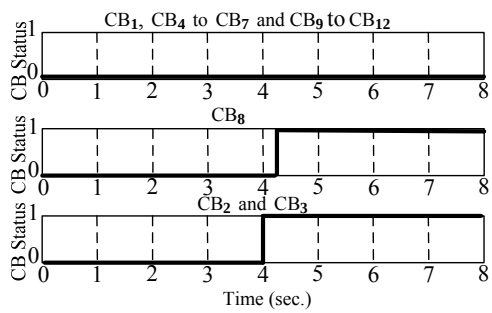

Fig. 12. Status of circuit breakers under normal condition when fault occurs in line 1.

which is equal to the total reactive power absorbed by the loads connected at bus B.

3) Fault on Line 1 during Normal Operation: The main objective of this scenario is to assure that the islanding protection and line protection schemes are coordinated properly. A three phase short circuit occurs on line 1 between bus A and bus B at t = 4 seconds when the utility power is connected. Fig. 10, Fig, 11 and Fig. 12 present the obtained simulation results. The DG is supplying 5 kW and zero reactive power and the ESS is operating under the floating condition prior to the fault. The over current protection relays the set of line 1 at the CB location CB_2 and CB_3 senses the faults and sends a signal to the circuit breaker CB_2 and CB_3 to open. After the disconnection of this line, a frequency deviation occurs on bus B and bus C. Since, the ESS is still connected to the utility, its frequency stabilizes in approximately less than 100 mili seconds. On the other hand, the DG still experiences a frequency deviation due to the excess loading on the DG. After a 300 mili seconds time delay, the frequency of the ESS stabilizes and the frequency of the DG still deviates. This indicates that the ESS is still connected to the utility while the DG is islanded. This is the second islanding condition (I_2). The CPU sends a signal to the DG to change its control from the unity power factor operation to the P-V control operation. In addition, a signal is sent to disconnect only the non-critical load connected to the DG i.e. L_2.

Since the interface control of the ESS is unchanged, the ESS still work under the floating mode. On the other hand, the interface control of the DG is changed and it supplies 2 kW and zero reactive power which is equal to the critical load (L_1) active and reactive power requirements. It takes less than 500 m sec for the voltage and frequency at bus B to stabilize within their standard values. It can be seen from Fig. 12 that circuit breaker CB_8 operates to disconnect the non-critical load L_2. An additional delay time of 200 m sec was used to provide a sufficient time for both the voltage and frequency to reach a stable condition.

4) Fault on Line 2 during Normal Operation: In this scenario, a three phase short circuit occurs on line 2 between bus A and bus C at t = 4 seconds when the utility power is connected. Fig. 13, Fig, 14 and Fig. 15 show the simulation results obtained for this scenario. Before the occurrence of the fault, the DG supplies 5 kW and zero reactive power and the ESS is operating under the floating condition.

The over current protection relays set at the end of line 2 (i.e. the relay at location CB_4 and CB_5) sense faults and send a signal to the circuit breakers CB_4 and CB_5 to isolate the faulty section. After the disconnection of line 2, a frequency deviation occurs on bus B and bus C. Since, the DG is still connected to the utility, its frequency stabilizes in less than 100 milliseconds. Meanwhile, the ESS still experiences a frequency deviation due to excess loading. After the 150 millisecond time delay, the frequency of the DG stabilizes and the frequency of the ESS still deviates. This indicates that the DG is still connected to the utility when the ESS is islanded. This is the third islanding condition (I_3). The CPU sends a signal to the ESS to change its control from unity power factor operation to P-V control operation. It also sends signals to trip CB_{10} to disconnect the non-critical load connected to the ESS.

Since the interface control of the DG is unchanged, it is still working under the PQ controlled mode. On the other hand, the interface control of the ESS is changed and it supplies 2 kW

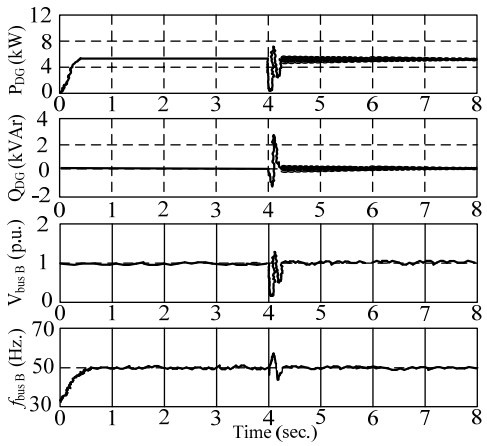

Fig. 13. Results of DG under normal condition when fault occurs at line 1for active power, reactive power, voltage and frequency at bus B.

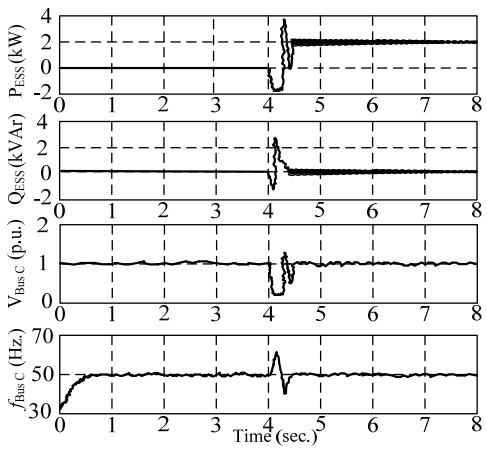

Fig. 14. Results of ESS under normal condition when fault occurs at line 1for active power, reactive power, voltage and frequency at bus C.

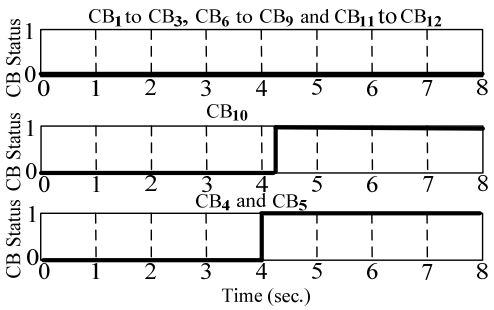

Fig. 15. Status of circuit breakers under normal condition when fault occurs in line 1.

and zero reactive power which is equal to the critical load (L_4) active and reactive power requirements. It takes time about 500 m sec for the voltage and frequency at bus C to stabilize to within their standard values. It can be seen from Fig. 15 that circuit breaker CB_{10} operates to disconnect the non-critical load L_4. An additional delay time of 250 m sec was used to provide sufficient time for both the voltage and the frequency to reach a stable condition.

5) Fault under Islanded Microgrid Operation: As stated earlier, during microgrid islanding operation (I_1), the DG operates in the P-V mode and the ESS operates in the P-Q mode. There is a possibility that a fault could occur on any of the lines during microgrid operation. The fault must be cleared and the DG and ESS should be controlled to operate in the P-V mode. Under this microgrid islanding fault condition, the DG and ESS are dedicated to supply only the critical loads connected to their respective buses. In order to explore this issue, the utility was disconnected at t = 3.5 seconds and three phase short circuit fault occurred at t = 6 seconds. Fig. 16, Fig. 17 and Fig. 18 present the simulation results for this condition.

As examined in this scenario (I_1), after 300 m sec from the moment of the microgrid occurrence, the CPU sends a signal to switch the DG to the P-V mode of operation and to disconnect the normal or non-critical loads. The total active power absorbed by the loads on the microgrid is 6 kW distributed among the three buses and 1 kVAR as reactive power. The microgrid maintains its stable operation until t = 6 seconds when a three phase short circuit occurs on any line (Line 1 or line 2) between bus A and bus B or bus C. After 100 m sec, the breakers (CB_2 and CB_3 for line 1 or CB_4 and CB_5 for Line 2) operate to disconnect the faulty section. As a result, two small islanded regions are produced (I_2 and I_3). Islanded region I_2 consist of the DG (operating in the P-V mode) and critical loads absorbing 4 kW of active power and 1 kVAR of reactive power. Islanded region I_3 consists of the ESS (operating in the P-Q mode) with 2 kW of active load. It can be seen from Fig.16 that the DG island frequency stabilizes at approximately 50 Hz in less than 150 m sec since it was previously operating in the islanded operation mode (P-V mode). On the other hand, the ESS island frequency stabilizes at a frequency that is outside the standard limits due to an excess in the load and due to the interface control design (unity power factor operation to the P-V mode).

To overcome this problem and for the survival of these two small islands, the CPU is designed to send a signal to disconnect the non-critical load (L_2) and to switch the ESS to the PV mode control. From Fig. 17, it can be seen that the ESS stabilizes. However, it does so at a frequency and voltage that are not within standard permissible levels due to the unity power factor operation of the ESS. At t = 6.3 seconds, the CPU takes suitable action by switching the ESS to the P-V mode. In addition, both the voltages and frequency of the ESS stabilize within the standard levels. When the DG and the ESS are operating as independent units as islands in the P-V mode, they only supply power to critical loads i.e. L_1 and L_4. The circuit breakers status is shown in Fig.18.

The simulation results show that the proposed control strategy is capable of differentiating between the different possible disturbances occurring during grid connected and microgrid operation. By properly coordinating the control and protection scheme, the nuisance tripping of the DG, the ESS and the non-critical load can be avoided while maintaining safe

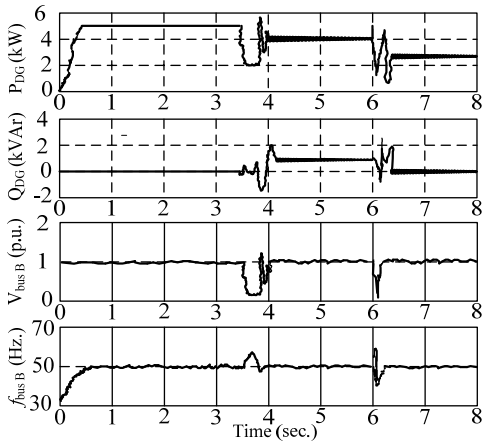

Fig. 16. Results of DG under microgrid condition when fault occurs at line 1for active power, reactive power, voltage and frequency at bus B.

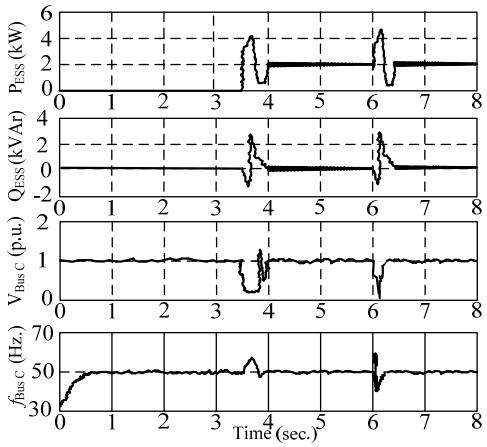

Fig. 17. Results of ESS under micro-grid condition when fault occurs at line 1 for active power, reactive power, voltage and frequency at bus C.

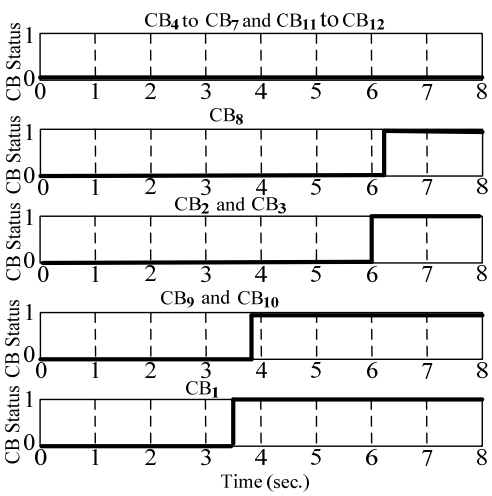

Fig. 18. Status of circuit breakers under microgrid condition when fault occurs in line 1.

islanded operation of the DG and the ESS.

B. Experimental Results

The proposed strategy was validated by experimental tests.

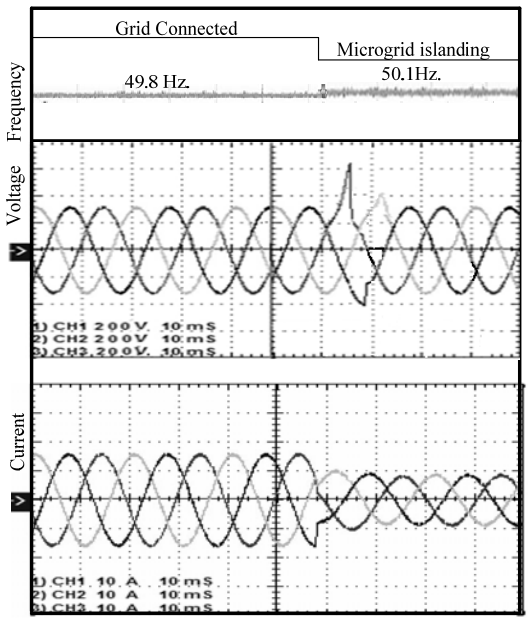

Fig. 19. Experimental results of micro-grid condition.

The algorithm shown in Fig. 3 was implemented in C++ in the Raspberry Pi2 modified version of Debian GNU/Linux. The core of the device is a Broadcom BCM2835 single board computer (SBC). It has a single core 700 MHz, ARM1176ZF-S processor and 512 MB of main memory. The voltages and currents are sensed using Hall Effect voltage and current transducers, LEM LV 25-P and LEM LA 55-P, and supplied to the SBC. Battery and photovoltaic emulators with their inverters are also connected to the grid. These inverters are commercial ones, with a modified configuration, in order to implement the proposed strategy. More precisely, the proposed droop method presented in Fig. 2, was programmed into the battery inverters, whiles the P-V power regulation scheme was programmed into the photovoltaic inverter.

The first test was conducted to validate the microgrid scenario. The experimental results are shown in Fig. 19 and they represent the grid connected and microgrid islanding condition (I_1). The voltage, current and frequency at the photovoltaic inverter before and after microgrid formation are shown. As a result, the battery and photovoltaic inverters shared the power in proportion to their ratings. The frequency was close to 50 Hz and the system was performing the microgrid operation. The second test validated the microgrid protection. In this scenario, the load connected at bus A (L_5) was switched on. As a result, the DG (photovoltaic emulator) and ESS (battery) supply more current than the set value. This enables the tripping of circuit breakers CB_2 and CB_3.

For this experimentation, power contactors ML 2 60947-4-1 are used as circuit breakers. As soon as the load L_5 is switched on, it creates an overload fault condition. In addition, the DG and ESS get separated and form two small islands as depicted in Fig. 20. The experimental results, shown in Fig. 20, represent the DG inverter currents, and the DG inverter bus

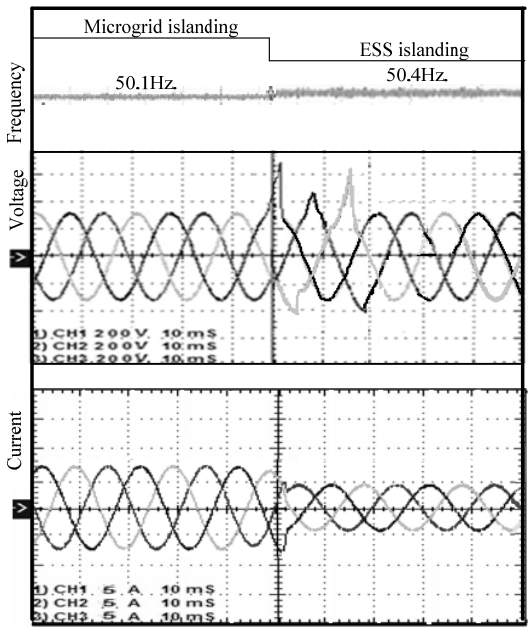

Fig. 20 Experimental results of ESS islanding condition.

voltage and frequency. At the beginning, both the DG and ESS currents were higher I_{DG} = 5.8 A and I_{ESS} = 1.9 A. Hence, the system operated in the microgrid islanding mode and the frequency was close to 50 Hz. At about 3 s, a L_5 = 2kW load was connected. The tripping of CB_2 and CB_4 took place. The DG and ESS currents were reduced and the system operated in separate DG and ESS islanding modes.

Since there were sudden reduction in the loads, the frequency continued to increase until it reached f = 50.4 Hz, when the system stopped in order to protect the batteries. The figure shows how the proposed strategy managed to either control the current of the DG or the ESS or to stop the system.

V. CONCLUSION

This paper investigates two challenging issues regarding the implementation of a microgrid, its control and protection. A control scheme is proposed to keep both the voltage and the frequency within their standard levels. Each DG and ESS is equipped with two interface controls, one for the grid connected and the other for islanded operation. A CPU is dedicated for managing the operation of the DG and ESS during different scenarios. The DG and ESS are equipped with islanding detection protection and the microgrid lines are protected using over current relays. The following conclusions can be drawn from the simulation and experimental results.

1. The DG must be able to supply reactive power during microgrid operation.

2. The battery backup should be sufficient for the survival of the islanding operation.

3. The islanding detection algorithm is a simple passive islanding scheme that relies on the voltage.

4. The over current relays should be properly coordinated to avoid unwanted tripping of the DG, the ESS or the load.

5. Further, the simulation and experimental results of the proposed controlled algorithm are compared and found to be satisfactory.

REFERENCES

[1] N. Kumar and S. Doolla, "Multiagent-based distributed energy resource management for intelligent microgrids," *IEEE Trans. Ind. Electron*., Vol. 60, No. 4, pp. 1678-1687, Apr. 2013.

[2] J.A. Pecas Lopes, N. Hatziargyriou, J. Mutale, P. Djapic, and N. Jenkins, "Integrating distributed generation into electric power systems: A review of drivers, challenges and opportunities," *Electric Power System Research*, Vol. 77, pp. 1189-1203, 2007.

[3] I. J.Balaguer, L. Qin, S.Yang, U. Supatti, and F. Z. Peng, "Control for grid connected and intentional islanding operations of distributed power generation," *IEEE Trans. Ind. Electron*., Vol. 58, No. 1, pp. 147-157, Jan. 2011.

[4] M. Sechilariu, B. Wang, and F. Locment, "Building integrated photovoltaic system with energy storage and smart grid communication," *IEEE Trans. Ind. Electron*., Vol. 60, No. 4, pp. 1607-1618, Apr. 2013.

[5] Q. Shafiee, C. Stefanovic, T. Dragicevic, P. Popovski, J. C. Vasquez, and J. M. Guerrero, "Robust networked control scheme for distributed secondary control of islanded microgrids," *IEEE Trans. Ind. Electron*., Vol. 61, No. 10, pp. 5363-5374, Oct. 2014.

[6] J. A. Peças Lopes, C. L. Moreira, and A. G. Madureira, "Defining control strategies for microgrids islanded operation," *IEEE Trans. Power Syst*., Vol. 21, No. 2, pp. 916-924, May 2006.

[7] F. Katiraei and M. R. Iravani, "Power management strategies for a microgrid with multiple distributed generation units," *IEEE Trans. Power Syst*., Vol. 21, No. 4, pp. 1821-1831, Nov. 2006.

[8] A. G. Tsikalakis and N. D. Hatziargyriou, "Centralized control for optimizing microgrids operation," *IEEE Trans. Energy Convers*., Vol. 23, No. 1, pp. 241-248, Mar. 2008.

[9] N. Hatziargyriou, H. Asano, R. Iravani, and C. Marnay, "Microgrids," *IEEE Power Energy Mag*., Vol. 5, No. 4, pp. 78-94, Jul./Aug. 2007.

[10] R. H. Lasseter, "Smart distribution: Coupled microgrids," *Proc. IEEE*, Vol. 99, No. 6, pp. 1074-1082, Jun. 2011.

[11] M. N. Marwali, J.-W. Jung, and A. Keyhani, "Control of distributed generation systems – Part II: Load sharing control," *IEEE Trans. Power Electron*., Vol. 19, No. 6, pp. 1551-1561, Nov. 2004.

[12] S. S. Khorramabadi and A. Bakhshai, "Intelligent control of grid-connected micro-grids: an adaptive critic-based approach," *IEEE Journal of Emergening and Selected Topics in Power Electronics*, Vol. 3, No. 2, pp. 493-504, Jun. 2015.

[13] H. H. Zeineldin, E. F. El-Saadany, M. M. A. Salama, "Impact of DG interface control on islanding detection and non detection zones," *IEEE Trans. Power Del*., Vol. 21, No. 3, pp. 1515-1523, Jul. 2006.

[14] J. He, Y. W. Li, and F. Blaabjerg, "An enhanced islanding micro-grid reactive power, imbalance power, and harmonic power sharing scheme," *IEEE Trans. Power Electron*., Vol. 30, No. 6, pp. 3389-3401, Jun. 2015.

[15] E. Serban, C. Pondiche, and M. Ordonez, "Islanding detection search sequence for distributed power generators under AC grid faults," *IEEE Trans. Power Electron*., Vol. 30, No. 6, pp. 3106-3121, Jun. 2015.
[16] J. M. Guerrero, P. C. Loh, T.-L. Lee, and M. Chandorkar, "Advanced control architectures for intelligent microgrids – Part I: Decentralized and hierarchical control," *IEEE Trans. Ind. Electron*., Vol. 60, No. 4, pp. 1254-1262, Apr. 2013.
[17] S. M. Brahma and A. A.Girgis, "Development of adaptive protection scheme for distribution systems with high penetration of distributed generation," *IEEE Trans. Power Del*., Vol. 19, No. 1, pp. 56-63, Jan. 2004.
[18] J. M. Guerrero, P. C. Loh, T.-L. Lee, and M. Chandorkar, "Advanced control architectures for intelligent microgrids – Part II: Power quality, energy storage, and AC/DC microgrids," *IEEE Trans. Ind. Electron*., Vol.60, No.4, pp. 1263-1270, Apr. 2013.
[19] A. Vaccaro, V. Loia, G. Formato, P. Wall, and V. Terzija, "A self-organizing architecture for decentralized smart microgrids synchronization, control, and monitoring," *IEEE Trans. Ind. Informat*., Vol. 11, No. 1, pp. 289-298, Feb. 2015.
[20] Z. Wang, B. Chen, J. Wang, M. M. Begovic, and C. Chen, "Coordinated energy management of networked microgrids in distribution systems, control, and monitoring," *IEEE Trans. Smart Grid*, Vol. 11, No. 1, pp. 45-53, Jan. 2015.
[21] H. Wan, K. K. Li, and K. P.Wong, "Multi-agent application of substation protection coordination with distributed generators," *European Transactions on Electrical Power*, Vol. 16, No. 5, pp. 495-506, Sep. 2006.
[22] K. A. Alobeidli, M. H. Syed, Mohamed S. El Moursi, and H. H. Zeineldin, "Novel coordinated voltage control for hybrid micro-grid with islanding capability coordinated energy management of networked microgrids in distribution systems, control, and monitoring," *IEEE Trans. Smart Grid*, Vol. 6, No. 3, pp. 1116-1127, May 2015.
[23] T. Logenthiran, R.T. Naayagi, W. L. Woo, V. T. Phan, and K. Abidi, "Intelligent control system for microgrids using multi-agent system," *IEEE Trans. Emerg. Sel. Topics Power Electron*., Vol. 3, No. 4, pp. 1036-1045, Dec. 2015.

Makarand Sudhakar Ballal was born in Nagpur, India. He received his B.E. degree in Electrical Engineering from Marathwada University, Aurangabad, India, in 1993; and his M.Tech. and Ph.D. degrees in Electrical Engineering from Nagpur University, Nagpur, India, in 1997 and 2007, respectively. From 1997 to 2012, he was with Maharashtra State Electricity Transmission Company Limited, Maharashtra, India, where he worked on commissioning, installation and testing of various types of HV and EHV electrical equipments and accessories. He was a Member of the research and development committee of Maharashtra State Electricity Transmission Company Limited, Maharashtra, India. He is presently working an Associate Professor in the Department of Electrical Engineering, Visvesvaraya National Institute of Technology, Nagpur, India. His current research interests include the condition monitoring and fault diagnosis of electrical machines.

Kishor V. Bhadane received his B.E. degrees in Electrical Engineering from the D. N. Patel College of Engineering, Shahada, India; and his M.E. degree in Electrical Engineering from the Government College of Engineering, Aurangabad, India. He is presently pursuing the Ph.D. degree at the Yeshwantrao Chavan College of Engineering (YCCE), Rashtrasant Tukadoji Maharaj Nagpur University, Nagpur, India. He is presently working as an Assistant Professor in the Department of Electrical Engineering, G. H. Raisoni Institute of Engineering and Management, Jalgaon, M. S., India. His current research interests include renewable energy sources, power quality, grid connected wind energy, custom power devices, etc.

Ravindra M. Moharil was born in Nagpur, Maharashtra, India, in 1966. Completed his B. E. from the Government College of Engineering, Karad, India, in 1989. Completed his Masters degree and Ph.D. degree in Renewable Energy from the Visvesvaraya National Institute of Technology (VNIT), Nagpur, India, in 1998 and 2009, respectively. He is presently working as a Professor in the Department of Electrical Engineering, Yeshwantrao Chavan College of Engineering, Nagpur, India. His current research interests include power systems and renewable energy.

Hiralal M. Suryawanshi was born in India, in 1963. He received his B.E. from Shivaji University, Kolhapur, India, in 1988. He received M.E. in Electrical Engineering from the Indian Institute of Science, Bangalore, India, in 1994; and his Ph.D. degree in Electrical Engineering from Nagpur University, Nagpur, India, in 1999. Since 2007, he has been an Professor in the Department of Electrical Engineering, Visvesvaraya National Institute of Technology, Nagpur, India. He is an Associate Editor of the IEEE Transactions on Industrial Electronics. His current research interests include power electronics and drives, and the condition monitoring of electrical equipment.